J Mater Sci: Mater Electron (2015) 26:2622–2628
DOI 10.1007/s10854-015-2733-9

Mechanical, microstructural and magnetic properties of the bulk BSCCO superconductor prepared by two different methods

S. Safran · A. Kılıç · E. Kılıçarslan · H. Ozturk · M. Alp · E. Asikuzun · O. Ozturk

Received: 4 December 2014 / Accepted: 19 January 2015 / Published online: 25 January 2015

Abstract BSCCO bulk samples have been prepared by solid-state reaction and ammonium nitrate precipitation methods with $Bi_{1.65}Pb_{0.35}Sr_2Ca_2Cu_3O_{10\pm y}$ stoichiometry. Structural, mechanical and magnetic characterizations of the samples were performed by the X-ray powder diffraction (XRD), the scanning electron microscopy (SEM), Microhardness measurements, AC susceptibility measurements. The XRD patterns showed that the diffraction peaks for our samples belong to the two main phase, namely 2223 and 2212 of the BSCCO. In this study we have focused on microhardness measurements to investigate the mechanical properties. Vickers microhardness, Young's modulus and yield strength values were calculated separately for all samples. In addition to these, we calculated the load independent hardness values of samples. Experimental results of hardness measurements were analyzed using the Meyer's law, proportional sample resistance (PSR) model, Elastic–Plastic deformation model (EPD) and indentation induced cracking (IIC) model. The critical transition temperature, phase purity, lattice parameter, surface morphology and crystallinity of the prepared bulk samples were compared with each other.

S. Safran (✉) · A. Kılıç · E. Kılıçarslan · H. Ozturk
Faculty of Science, Department of Physics, Ankara University, Ankara, Turkey
e-mail: safranserap@gmail.com; safran@science.ankara.edu.tr

S. Safran · A. Kılıç · E. Kılıçarslan · H. Ozturk · M. Alp
Center of Excellence for Superconductivity Research, Ankara University, Ankara, Turkey

E. Asikuzun · O. Ozturk
Department of Physics, Kastamonu University, Kastamonu, Turkey

1 Introduction

Since the discovery of the Bi-based high-temperature ceramic superconductors; many researches have been carried out to characterize properties of the materials [1–11]. Preparation method, chemical doping, substitution, addition and diffusion play a very important role on critical superconducting parameters of the high-T_c superconductors. Enhancing the mechanical properties are significant goal of the studies in the field of Bi-based superconductors for their use in engineering applications. Especially practical applications are restricted because of brittleness of materials. The mechanical behavior of the BSCCO can be severely affected by defects, dislocation, twins, micro cracks and pores. To the best of our knowledge, previous studies mostly reported on the effects of mechanical properties of some materials substitution in BSCCO [12, 13].

The behavior of materials under mechanical loads is called as "mechanical properties". The mechanical properties are mainly resulted from the bond strength between atoms. However, there is the effect of the inner structure of material (microstructure). So that it becomes possible to obtain different mechanical properties in the same material by changing the internal structure. In addition, hardness is the resistance against a solid object which is immersed in the surface of a material. Hardness values are a great important because these are directly related to strength of materials. It can be measured non-destructively. Hardness test is a test method which is relative values about the strength of the material. According to the geometry of indenter and size of the applied load, hardness testing methods are called as Brinell, Vickers and Rockwell hardness testing method.

We aimed to study the effects of different preparation methods on mechanical, structural and magnetic properties

of BSCCO system with general formula $Bi_{1.65}Pb_{0.35}Sr_2Ca_2Cu_3O_{10\pm y}$. In this study, the samples were prepared by a conventional solid state method (SS) and ammonium nitrate precipitation method (AN).

2 Experimental

Superconducting samples with chemical composition $Bi_{1.65}Pb_{0.35}Sr_2Ca_2Cu_3O_y$ were prepared by solid state reaction method and ammonium nitrate precipitation methods from the powders of Bi_2O_3, PbO, $SrCO_3$, $CaCO_3$ and CuO with purities of more than 99.9 %. The powders were mixed in the appropriate amounts and ball-milled 3 h at 75 rpm. The milling procedure was maintained in a tungsten carbide jar together with tungsten carbide balls. The mixture was calcinated at 775 °C for 12 h. After the first calcination, the powders were grinded by using ball milling with same procedure. Then the mixture was calcinated at 810 °C for 24 h. Powders were pressed into pellets with 1 × 3 × 12 mm dimensions under the pressure of 5 tonnes. Pellets were annealed at 845 °C in air for 96 h. The furnace was heated to the annealing temperature with 1 °C/min heating rate. Then 1 °C/min rates were applied after the heat treatment. However, to obtain chemically homogenous mixture, appropriate amount of ammonium nitrate was added to the milled powders and heated at 250 °C for the ammonium nitrate precipitation methods. The other procedure is same for two methods. According to preparation methods, the pellets were called B and D for SS and AN, respectively.

Our samples have been investigated by means of XRD, Microhardness, SEM and AC susceptibility measurements. XRD data were taken using a Rigaku D/Max-IIIC diffractometer with CuK_α radiation in the range $2\theta = 3$–60 with a scan speed of 3 °/min and a step increment of 0.02. Vickers microhardness measurements are conducted at room temperature in air by using a digital microhardness tester (SHIMADZU HVM-2) to obtain information about the mechanical properties of the BSCCO samples prepared at different conditions. A rigid Vickers pyramidal indenter is applied for 10 s using different load in the range from 0.245 to 2.940 N and the diagonals of indentation are measured with an accuracy of ±0.1 μm. The Vickers microhardness measurements are performed with an average of 10 readings at different locations of sample surfaces to obtain reasonable mean values for each applied load. The microhardness measurements are analyzed by means of various models. Microstructure examinations were performed using a Jeol JSM-5300 SEM. Samples were prepared in the normal manner for SEM measurements, ground on 2,400 grit, and polished on 0.5 and 0.1 μm alumina lap wheels. The samples were coated with a thin layer of gold to avoid the charging effect for SEM examinations. Polished surfaces of the samples were investigated using a SEM. The susceptibility measurements were carried out by a commercial Lake Shore 7130-model ac susceptometer employing a mutual inductance coil system with a closed cycle refrigerator.

3 Results and discussion

XRD patterns, which demonstrate phase formations of the B and D of BSCCO samples annealed at 845 °C in air for 96 h are shown in Fig. 1. The detected major phases are Bi-2223 and Bi-2212, with the fraction of the latter being higher. Traces of non-superconducting Ca_2PbO_4 and one unknown phase is also detected in all samples. The relative volume fractions of the Bi-2223 and Bi-2212 phases in all the samples were estimated from the peak heights of the reflections belonging the same particular crystallographic plane, using the following well-known expressions [14, 15]:

$$f_{(2223)} = \frac{\sum I_{H(hkl)}}{\sum I_{H(hkl)} + \sum I_{L(hkl)}} \quad (1)$$

$$f_{(2212)} = \frac{\sum I_{L(hkl)}}{\sum I_{H(hkl)} + \sum I_{L(hkl)}} \quad (2)$$

Here $I_H(hkl)$ and $I_L(hkl)$ are the intensities of the (hkl) diffraction lines for Bi-2223 and Bi-2212 phases (Fig. 1). There is no effective differences in the volume fractions of the samples prepared by two methods. The lattice parameters of the samples were performed employing the least-squares method and using the data extracted from XRD measurements. The results are listed in Table 1. It is

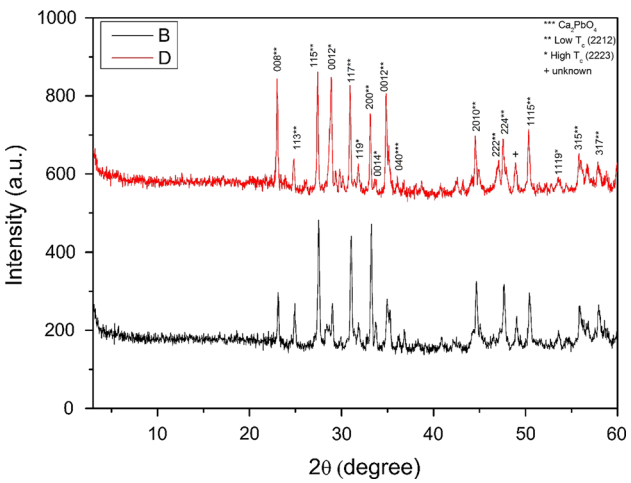

Fig. 1 XRD patterns of the B and D samples annealed at 845 °C in air for 96 h

observed that D sample prepared by AN has higher peak intensity than B sample prepared by SS.

In this study, the Vickers hardness test is used. During the test, five different loads (0.245, 0.490, 0.980, 1.960, 2.940 N) are applied on the sample surface by the indenter with 10 s. Vickers hardness values are calculated using diagonal length of trace formed on the surface of the sample after removing the indenter by using Eq. 3.

$$H_v = 1854.4\frac{F}{\left(\frac{d_1+d_2}{2}\right)^2} \quad (3)$$

Materials exhibit two types behavior as *ISE* and *RISE*. While *ISE* is defined as hardness decreases with increasing applied load, *RISE* is defined as hardness increases with increasing applied load. The variation graph of hardness against the applied load is given in Fig. 2. As can be seen from the graph, hardness values increased with increasing the applied load to 0.245 N from 2.940 N. This means that the material shows *RISE* behavior. As well as applied load, hardness of material has been affected by the preparation method. Hardness of D sample is higher than B sample. Moreover, there is reached to plateau region around 1.5 N. A significant change in the hardness values was not observed over 2 N. The load dependent elastic modulus (E) and the yield strength (Y) values of material are calculated (Table 2). E and Y values increase with increasing the applied load.

There are models used in microhardness analysis of materials. The results obtained from these models are described below.

3.1 Meyer law

Meyer Law is the most fundamental law that is used to definition of mechanical behavior exhibited by material [16].

$$F = Ad^n \quad (4)$$

The n value is obtained from slope of *InF-Ind* graph (Fig. 3) determines the behavior of the material (*ISE* or *RISE*). If n is smaller than 2, the material exhibits *ISE* behavior. But this value is greater than 2, the material exhibits *RISE* behavior [17, 18]. In this study, n values are greater than 2 for the samples B and D (Table 3). According to these results, it is understood that both of the samples show *RISE* behavior.

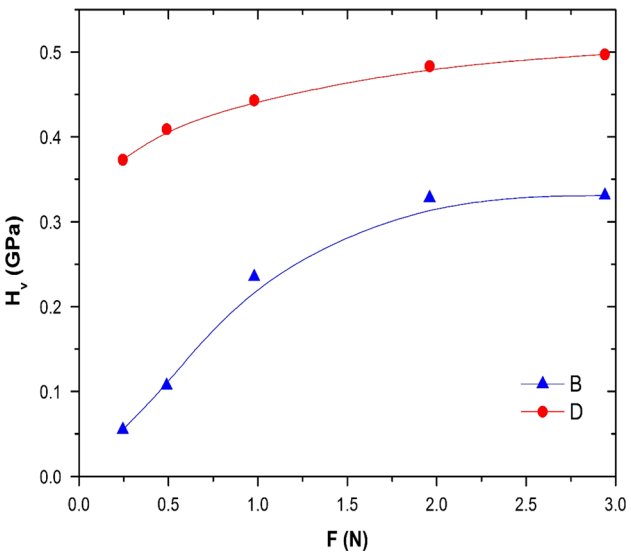

Fig. 2 Variations of microhardness with load for the samples

Table 2 Load dependent H_v, E and Y values of the B and D samples

Samples	F (N)	H_v (GPa)	E (GPa)	Y (GPa)
B	0.245	0.055	4.507	0.018
	0.490	0.107	8.770	0.035
	0.980	0.235	19.26	0.078
	1.960	0.328	26.88	0.109
	2.940	0.331	27.12	0.110
D	0.245	0.373	30.57	0.124
	0.490	0.409	33.52	0.136
	0.980	0.443	36.30	0.147
	1.960	0.483	39.58	0.161
	2.940	0.497	40.73	0.165

3.2 PSR (proportional sample resistance) model

The load independent H_{PSR} values are calculated using the β value that is obtained from slope of *F/d–d* graph (Fig. 4) is drawn using Eq. 5.

$$\frac{F}{d} = \alpha + \beta d \quad (5)$$

$$H_{PSR} = 1854.4\beta \quad (6)$$

Table 1 Lattice parameters, volume fraction and T_c data of $Bi_{1.85}Pb_{0.35}Sr_2Ca_2Cu_3O_y$

Sample name	Lattice parameters (Å)		Volume fraction (%)		T_c^{onset} (K)	Preparation technique
	a	c	Bi-2223	Bi-2212		
B	5.431	30.726	13	87	106.7	SS
D	5.452	30.739	17	83	108.0	AN

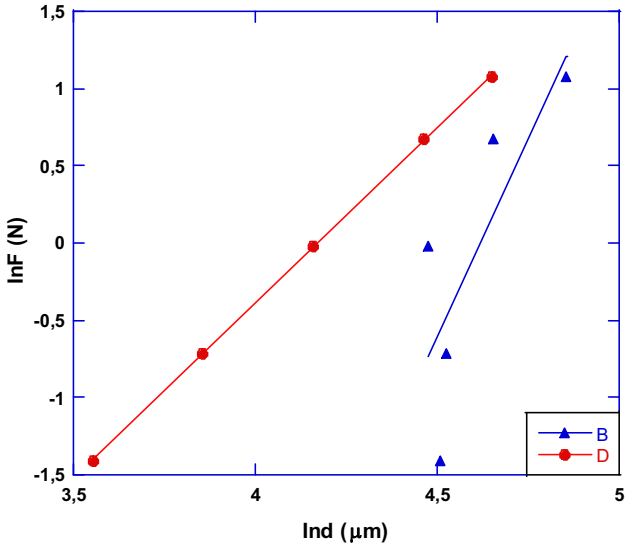

Fig. 3 Variation of applied load lnF with diagonal lnd for the samples

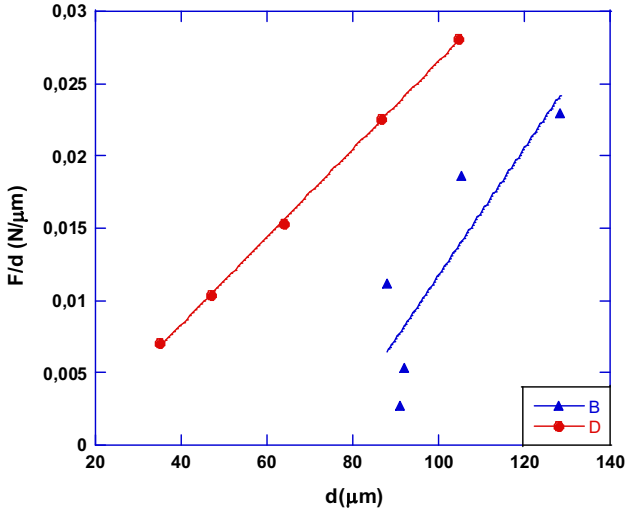

Fig. 4 Plots of *F/d* versus *d* for the samples

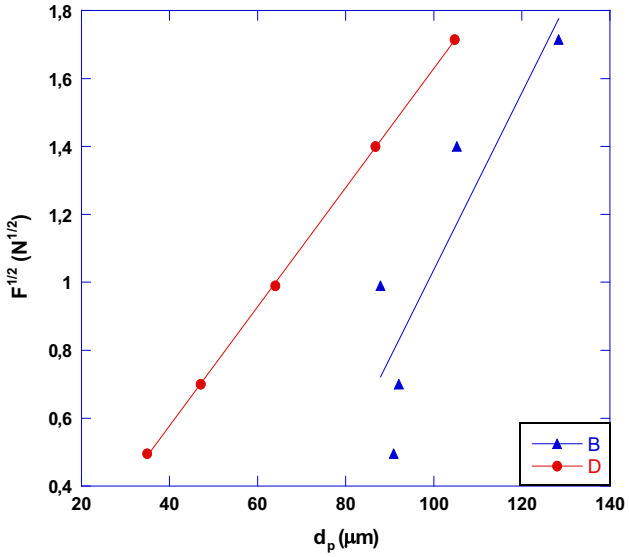

Fig. 5 Plots of square root of applied loads versus diagonal length for the samples

It can be seen that α value is defined as energy of cracks formed on the surface of the sample is negative for B and D (Table 3). The reason for this is materials that have *RISE* behavior. If the material has *ISE* behavior, α value is positive [19].

Hardness values are calculated according to *PSR* model are so far from plateau region or load dependent hardness values. This means that the *PSR* model is not suitable for the hardness analysis of materials produced in this study.

3.3 Elastic/plastic deformation (EPD) model

In the elastic plastic deformation (*EPD*) model, the type of the deformation formed in material is determined [20, 21]. d_e value is point where the graph (Fig. 5) intercepts the y-axis is the coefficient of elastic deformation. If d_e value is negative, elastic deformation is not observed in the material. There is only plastic deformation. If d_e value is positive, there is elastic deformation as well as plastic deformation. In general, elastic deformation coefficient of materials that exhibit the *ISE/RISE* behavior is positive/negative.

$$F = B\left(d_{\mathrm{p}} + d_{\mathrm{e}}\right)^2 \tag{7}$$

$$H_{\mathrm{EPD}} = 1854.4\mathrm{B} \tag{8}$$

As seen from Table 4, elastic deformation coefficient (d_e) is negative in both B and D. This means that the materials exhibit the *RISE* behavior. This case confirms the results obtained until now. Hardness values are calculated according to *EPD* model are so far from plateau region. So, *EPD* model is insufficient for the microhardness analysis.

Table 3 *n* values of the samples according to Meyer's Law and best-fit results of experimental data according to *PSR* model for B and D samples

Samples	$\alpha \times 10^{-3}$ (N)	$\beta \times 10^{-5}$ (N/μm)	H_{PSR} (GPa)	H_V (GPa)	*n*
B	−32.22	43.96	0.86	0.234–0.331	5.12
D	−3.82	30.36	0.562	0.443–0.497	2.26

3.4 Indentation-induced cracking (IIC) model

The IIC model is used in hardness analysis of materials that show *RISE* behavior [22–24]. According to this model, the applied test load is equilibrated by the total sample resistance in maximum depth. This resistance is composed of four components.

1. Shift of the indenter or sample at the interface
2. Elastic Deformation
3. Plastic Deformation
4. Cracks of sample

Hardness values are calculated using Eq. 9 in this model.

$$H_v = K\left(\frac{P^{5/3}}{d^3}\right)^m \quad (9)$$

m value is determined from slope of $In(F^{5/3}/d^3)$–InH_v graph (Fig. 6) is used to determination of behavior of material (*ISE* or *RISE*). If m is greater than 0.6 the material has a normal *ISE* behavior. But if m is less than 0.6, it has a *RISE* behavior [25, 26]. m values are 0.58 and 0.34 for B and D sample, respectively. So, materials have *RISE* character. Regression analysis of experimental data according to IIC Model is given in Table 5. Compared to the values are calculated using the other models, the microhardness values calculated from *IIC* model are quite similar to the microhardness values in the plateau region (Table 6). Therefore, *IIC* model is the most suitable model to use in the microhardness analysis.

Figure 7 shows surface micrographs of the prepared samples. It is observed that the microstructures of B and D samples exhibit a common feature of plate-like and strip-like grains, respectively. The grains are randomly distributed. Although the grain size of B is relatively bigger than the other sample, it may be said that D sample has comparatively denser surface structure. These surface structures are compatible with the microhardness results. As shown in Fig. 7, the sample D has less porosity from the B sample. Hardness is a measure of porosity. Smaller values of hardness are obtained where porosity is high. The results of the hardness values are consistent with the SEM measurements.

In Fig. 8, we have plotted the normalized ac susceptibility curves as a function of temperature at $H_{ac} = 640$ A/m, frequency $f = 125$ Hz. Note that there exists two-step change to full diamagnetism in-phase component of the fundamental susceptibilities, χ', of two samples. The first drop, near $T_{c,}$ corresponds to 2223 phase; another drop at low temperatures indicates to 2212 phase. The out-of-phase component, χ'', exhibits two peaks with decreasing temperature. $T_{c,}^{onset}$ value is given in Table 1.

Table 4 Best-fit results of experimental data according to *EPD* model for B and D samples

Samples	d_e (μm)	$B^{1/2}$ (GPa)	H_{EPD} (GPa)	H_v (GPa)
B	−1.57	0.0261	1.263	0.234–0.331
D	−0.123	0.017	0.535	0.443–0.497

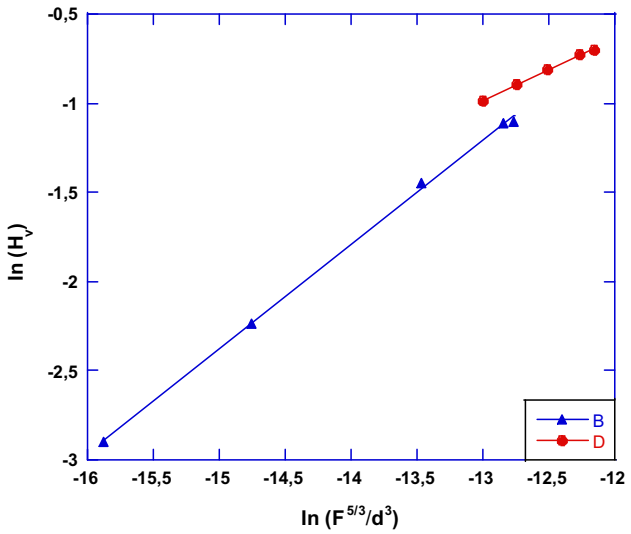

Fig. 6 Plot of lnH_V against $ln(F^{5/3}/d)^3$ according to IIC model for all the samples

Table 5 Regression analysis of experimental data according to *IIC* Model

Samples	*m*	K ($N^{(3-5m)/3}$/ $\mu m^{(2-3m)}$)	H_{IIC} (GPa)	HV (Plateau region) (GPa)
B	0.58	595.85	0.224	0.234–0.331
D	0.34	31.81	0.450	0.443–0.497

Table 6 The results of load dependent Vickers microhardness at the plateau region and load independent hardness values calculated using *PSR*, *EPD* and *IIC* models

Samples	H_{PSR} (GPa)	H_{EPD} (GPa)	H_{IIC} (GPa)	H_v (GPa)
B	0.815	1.263	0.224	0.234–0.331
D	0.562	0.535	0.450	0.443–0.497

4 Conclusion

Microhardness measurements were performed to determine the mechanical properties of the samples. In order to determine the most suitable model, Meyer's law, *PSR* model, *EPD* model and *IIC* model were applied to hardness values of the samples. In addition to these structural properties were obtained with XRD and SEM measurement. Also the magnetic characterizations of the samples

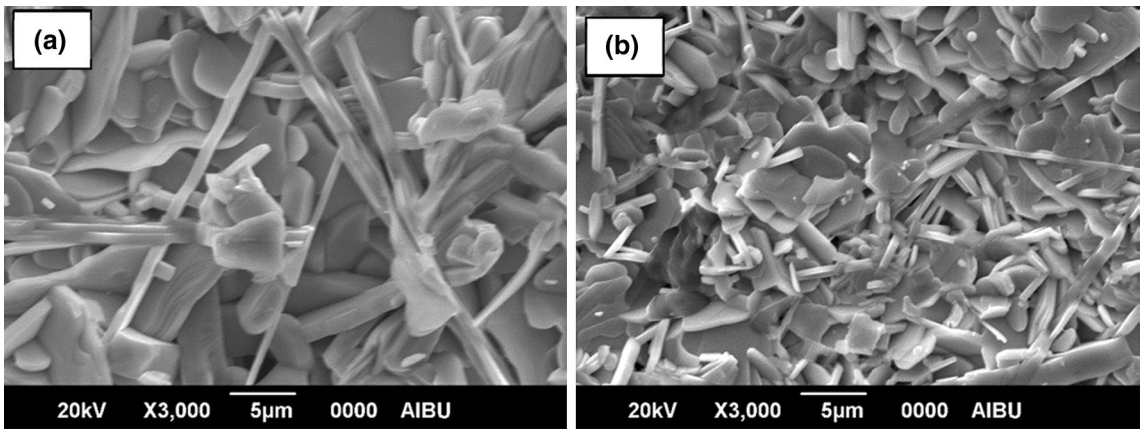

Fig. 7 Surface micrographs of the (**a**) B and (**b**) D sample

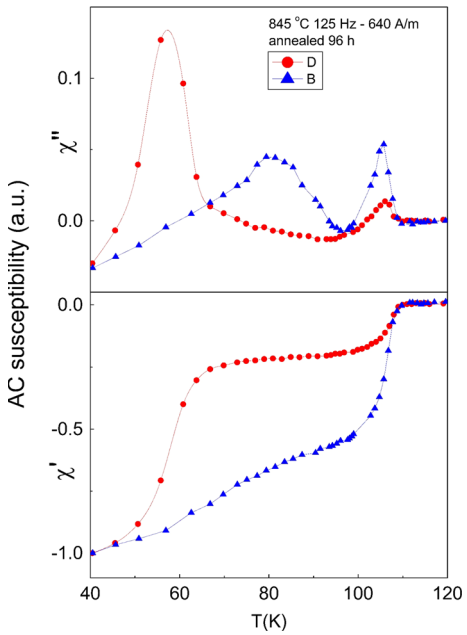

Fig. 8 Plot of real (χ') and imaginary (χ'') components of AC susceptibility as a function of temperature for B and D sample

were performed AC susceptibility measurements. The following results are obtained;

- Mechanical, structural and magnetic properties of the BSCCO superconductors with the measurements were determined to be strongly dependent on the fabrication methods.
- According to the Vickers microhardness measurement, it is seen that the microhardness values of the samples that are produced in different methods are depend on the load applied.
- The hardness of all samples increased with increasing applied loads. This behavior is referred to as *RISE* in the literature.
- Also the sample prepared by ammonium nitrate precipitation method was found to be harder than the sample prepared by solid state reaction method.
- *IIC* model is determined as the most successful model describing the mechanical properties of our samples.
- The hardness results were confirmed by SEM and XRD measurements.
- T_c^{onset} values were obtained by the Ac susceptibility measurements.

Acknowledgments This work has been supported by Turkish Research and Scientific Council (TUBITAK) under Grant contract No: 113F150. We also acknowledge The Republic of Turkey, Ministry of Development under the Project Number 2010K120520.

References

1. N. Ghanzanfari, A. Kılıç, A. Gencer, H. Özkan, Solid State Commun. **144**, 210 (2007)
2. C. Terzioglu, M. Yilmazlar, O. Ozturk, E. Yanmaz, Phys. C **423**, 119 (2005)
3. C. Terzioglu, O. Ozturk, A. Kilic, A. Gencer, I. Belenli, Phys. C **434**, 153 (2006)
4. S.M. Khalil, J. Phys. Chem. Solids **64**, 855 (2003)
5. A. Biju, R.P. Aloysius, U. Syamaprasad, Supercond. Sci. Technol. **18**, 1454 (2005)
6. N. Udomkan, P. Vinotai, R. Suryanarayanan, N. Charoenthai, Supercond. Sci. Technol. **18**, 1294 (2005)
7. K. Ozturk, S. Celik, U. Cevik, E. Yanmaz, J. Alloys Compds. **433**, 46 (2007)
8. A. Biju, R.G. Abhilash Kumar, R.P. Aloysius, U. Syamaprasad, Phys. C **449**, 109 (2006)
9. V.G. Prabitha, A. Biju, R.G. AbhilashKumar, P.M. Sarun, R.P. Aloysius, U. Syamaprasad, Physica C **433**, 28 (2005)
10. M. Yilmazlar, O. Ozturk, O. Gorur, I. Belenli, C. Terzioglu, Supercond. Sci. Technol. **20**, 365 (2007)
11. N. Güçlü, A. Kılıç, I.N. Askerzade, A. Gencer, Phys. Stat. Sol. **201**, 995 (2004)
12. M. Yilmazlar, H.A. Cetinkara, M. Nursoy, O. Ozturk, C. Terzioglu, Phys. C **442**, 106 (2006)

13. A. Tampieri, G. Celotti, S. Guicciardi, C. Melandri, Mater. Chem. Phys. **42**, 188 (1995)
14. C.W. Chiu, R.L. Meng, L. Gao, Z.J. Huang, F. Chen, Y.Y. Xue, Nature **365**, 323 (1993)
15. S.A. Halim, S.A. Khawaldeh, S.B. Mohammed, H. Azhan, Mater. Chem. Phys. **61**, 251 (1999)
16. D. Tabor, The hardness and strength of metals. J. Inst. Met. **79**, 1–18 (1951)
17. H. Koralay, A. Arslan, S. Cavdar, O. Ozturk, E. Asikuzun, A. Gunen, A.T. Tasci, J. Mater. Sci.: Mater. Electron. **24**(11), 4270–4278 (2013)
18. O. Ozturk, M. Coskunyurek, E. Asikuzun, N. Soylu, A. Hancerliogullari, A. Varilci, C. Terzioglu, J. Mater. Sci.: Mater. Electron. **25**(1), 444–453 (2014)
19. E. Asikuzun, O. Ozturk, H.A. Cetinkara, G. Yildirim, A. Varilci, M. Yılmazlar, C. Terzioglu, J. Mater. Sci.: Mater. Electron. **23**, 1001–1010 (2012)
20. S.J. Bull, T.F. Page, E.H. Yoffe, Phil. Mag. Lett. **59**, 281 (1989)
21. G.P. Upit, S.A. Varchenya, Phys. Status Solidi A **17**, 831 (1966)
22. L. Arda, O. Ozturk, E. Asikuzun, S. Ataoglu, Powder Technol. **235**, 479–484 (2013)
23. M. Tosun, S. Ataoglu, L. Arda, O. Ozturk, E. Asikuzun, D. Akcan, O. Cakiroglu, Mater. Sci. Eng., A **590**, 416–422 (2014)
24. S. Safran, E. Asikuzun, E.S. Kilicarslan, A. Kilic, O. Ozturk, A. Gencer, J. Mater. Sci.: Mater. Electron. **25**, 2737–2747 (2014)
25. R. Awad, A.I. Abou-Aly, M. Kamal, M. Anas, J. Supercond. Nov. Magn. **24**, 1947–1956 (2011)
26. K. Sangwal, Mater. Chem. Phys. **63**, 145–152 (2000)